Fachtagung "Experimentelle Strömungsmechanik"
3. – 5. September 2019, Erlangen

Steady three-dimensinal free-surface patterns in gravity-driven film flow over a sinusoidal bottom contour

B. Al-Shamaa[1] and A. Wierschem[1,2]
[1]Institute of Fluid Mechanics, Friedrich-Alexander-Universität Erlangen-Nürnberg (FAU), Cauerstr. 4, 91058 Erlangen, Germany
[2]LSTME Busan, 1276 Jisa-Dong, Gangseo-Gu, Busan 46742, South Korea

Key words: **film flow, free-surface detection, light-sheet technique, pattern formation**

Abstract

The current work is an experimental study on stable steady three-dimensional free-surface patterns that occur during the film flow over an inclined sinusoidal channel. The patterns are studied using shadowgraphy and light-sheet imaging, see Wierschem and Aksel, 2004. The range of Reynolds number studied was between 8 and 43. In this range of Reynolds numbers, the formation of the three dimensional patterns on the free surface occur.

Introduction

Gravity driven film flow over undulated substrates has a wide range of industrial and environmental applications, for instance, in heat and mass transfer equipment such as falling film evaporators and condensers (Bontozoglou and Papapolymerou, 1997), in coating process, biomedical flows (Schörner et al. 2016), heat exchangers, and many other applications (Wierschem et al. 2010). In the case of film flow over a sinusoidal profile surface, the wavelength of the profile has a strong influence on the free surface response. Apart from linear and nonlinear resonance of the free surface with the bottom undulation (e.g. Wierschem et al. 2008, Heining et al. 2009), the profile may cause eddies in the troughs (e.g. Wierschem et al. 2003), hydraulic jumps (e.g. Wierschem and Aksel, 2004) and may alter the primary instability of the steady flow (e.g. Wierschem et al. 2005). However, features of the bottom contour hidden by eddies hardly affect the free surface (M. Schörner, D. Reck, N. Aksel, 2015). Aksel and Schörner, 2018, provide a recent overview on the impact of topography on film flow. The present work focusses on the formation of three-dimensional patterns of the free film-surface.

Experimental setup

The studied system consists of an inclined open channel with a length of 950 mm and a width of 170 mm. The channel has transparent Plexiglas sidewalls and an aluminum bottom that has a sinusoidal contour in streamwise direction with a wavelength λ = 10 mm and an amplitude α = 1 mm (as shown in Figure 1). The inclination angle θ of the channel was kept constant for all experiments at a value of 15°.

Copyright © 2019 and published by German Association for Laser Anemometry
GALA e.V., Karlsruhe, Germany, ISBN 978-3-9816764-6-4

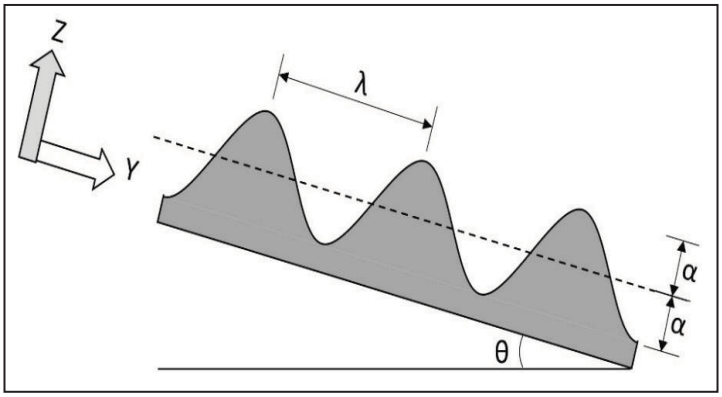

FIG. 1. Bottom contour of the inclined channel. Wavelength λ: 10 mm; amplitude α: 1 mm, inclination angle θ: 15°.

The working fluid for all runs was a silicon oil (ELBESIL ÖL B10). It has a density of 0.96 g/cm³ and a kinematic viscosity of 10.3 mm²/s at a temperature of 298.15 K. The experimental setup also consists of a storage tank for the silicon oil. Its temperature was controlled with a Thermo Haake C25P thermostat. For all tests, the temperature of the silicon oil was kept constant during the run at 297.15 K. Two digital thermometers were installed at the inlet and the exit of the channel for monitoring any change in the film temperature, in all the experiments it was kept in the range of constant temperature condition ±0.3K. An eccentric worm pump was used to pump the silicon oil from the storage tank to the top of the inclined channel. The pumping speed and thus the flow rate was frequency controlled.

Before initiating our experiments, the relationship between the pumping frequency and the Reynolds number was established at a constant temperature of 297.15 K. For each pumping frequency, silicon oil flowing down the channel was collected in a big beaker. The time to fill the beaker was measured using a stop watch and the collected mass was measured with an electronic balance. To exclude wall friction effects, measurements were carried out with a gate of 30 mm width, which was fixed in the middle of the channel exit. For each pumping frequency, the mass flow rate was measured three times and the average of them was calculated. The kinematic viscosity of the silicon oil was measured an Ubbelohde capillary viscometer at the same temperature. The density of the silicon oil was measured using a Mohr balance at the same temperature. According to the flow rates, we covered a Reynolds number range between 8 and 43, where the Reynolds number Re is defined with the average film velocity in the center of the channel: $Re = \rho V / (\eta b)$, where ρ and η indicate liquid density and dynamic viscosity. V is the flow rate of the liquid flowing through the gate of width b.

We visualized the free-surface pattern with shadowgraphy. Therefore, we placed a camera (max. frame rate: 15 fps; resolution: 1280 x 1024 pixel) perpendicular to the inclined channel to capture the top view of the free-surface pattern. The camera captured an area that is approximately 210 mm long and covered the entire width of the channel. The setup is sketched in Figure 2.

Shadowgraphy allows detecting large-scale properties of the pattern, regularity, intensity distributions and wavelengths of the pattern. Yet, since the shadowgraph contrast is rather sensitive to the second derivative of the surface elevation, its double integration makes it difficult to determine the precise surface elevation, see e.g. Wierschem and Linde, 2013 and Schöpf, et al. 1996, we used a light-sheet technique to quantify the surface shape and pattern amplitudes. Similar to Wierschem and Aksel, 2004, we generated a laser-light sheet in main flow direction and captured to light scattered from the liquid in light sheet into a camera (frame rate: 25 fps; resolution: 1280 x 1024 pixel). To provide a view on the free surface in the light sheet undisturbed by meniscus or surface undulations, this camera was inclined by 15° with respect

Copyright © 2019 and published by German Association for Laser Anemometry
GALA e.V., Karlsruhe, Germany, ISBN 978-3-9816764-6-4

to the spanwise direction of the channel, see Figure 2. Different from Wierschem and Aksel, 2004, we did not use fluorescent tracers as indicators of the liquid film. Yet, for the rather small scales relevant in our current study, using tracers would result in a rather coarse image of the free surface. Instead, like Schörner et al, 2015, 2016, we added the dye Quinizarin (Q906-100G ALDRICH Chemistry). It mixes well with the silicon oil and fluoresces in the red-orange. To excite fluorescence, we used a blue laser (wavelength: 450 nm; power: 40 mW). A color filter was placed in front of the camera lens to image the fluorescent light while suppressing the blue light that is strongly scattered particularly from the bottom contour. Camera and laser were both fixed to the same traverse to enable simultaneous displacement for scanning the area of interest. The pictures were calibrated by imaging scaled paper in the empty channel. The light-sheet study was carried out in a specific area of the bottom contour that has the dimensions of 30 mm length and 17 mm width. This area is 130 mm downstream from the inflow and 4 mm from the sidewall. It contains three crests and two troughs of the bottom topography, the light-sheet projection on the bottom contour has width of 1 mm approximately, see Figure 3.

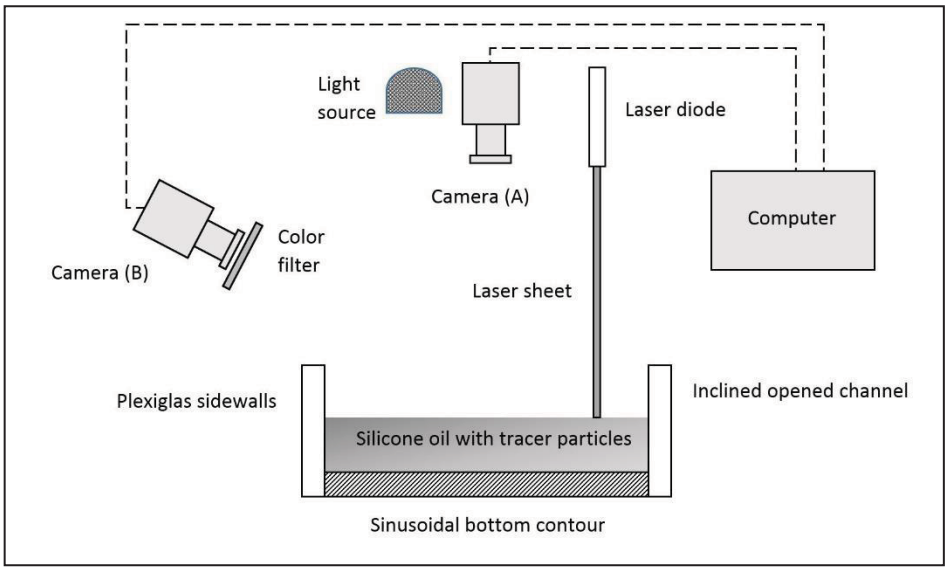

FIG. 2. Experimental setup and camera configuration

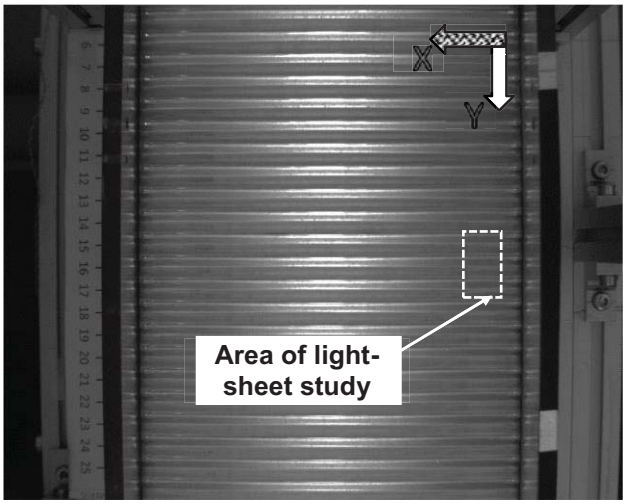

FIG. 3. Top view of the channel

Copyright © 2019 and published by German Association for Laser Anemometry
GALA e.V., Karlsruhe, Germany, ISBN 978-3-9816764-6-4

In the light-sheet study, a MATLAB edge detection program was used to detect the free surface position. Input data of the program were videos captured with the inclined camera. In order to ensure a reliable edge detection with reduced processing time the program uses several steps:

1. The image captured was converted from color RGB to grayscale. Although we used a black and white camera, this filter was necessary because the frames extracted from the videos had RGB format.
2. An unsharp filter is applied to the grayscale image followed by an average filter.
3. The resulting image was treated with a 5x11 median filter.
4. Thereafter, a close operation was applied and the image was binarized according to determined threshold.
5. An opening operation was applied to the resulting image. It removes small objects and otherwise reverts the closing operation.
6. Finally, the bright line is extracted and evaluated.

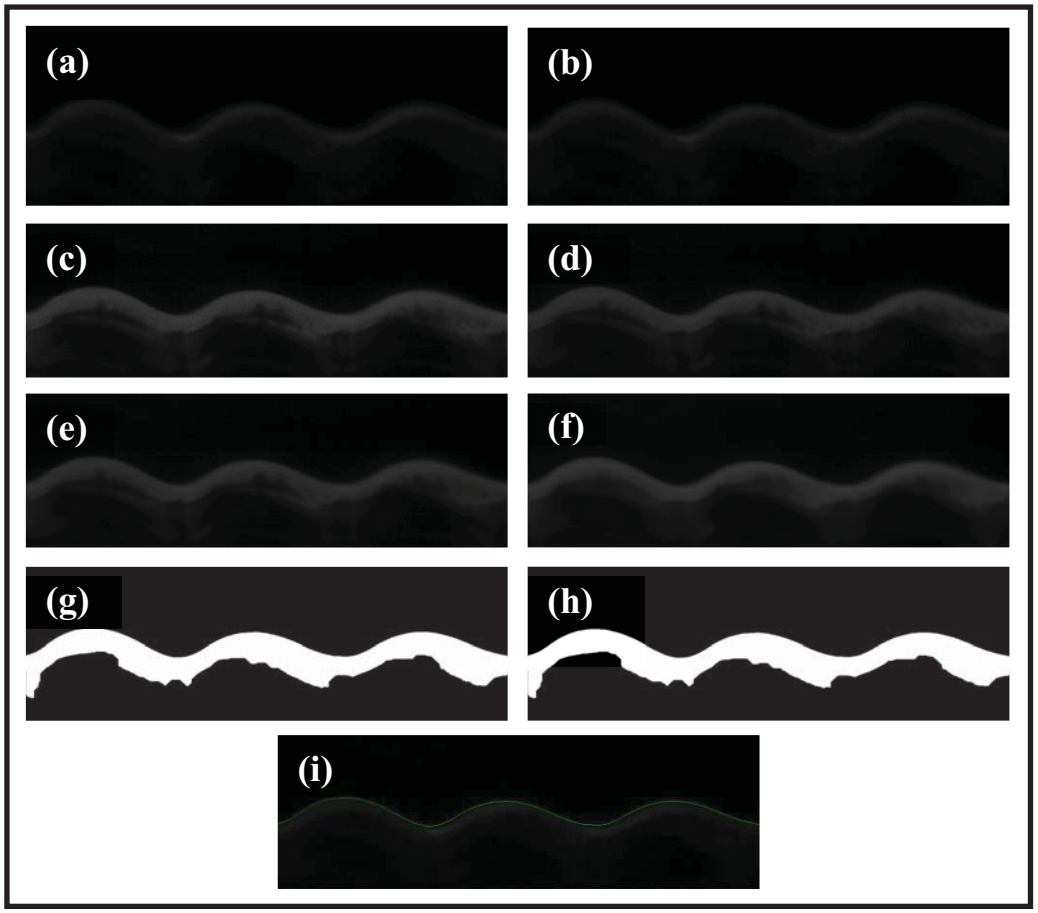

FIG. 4. MATLAB edge detection program steps. (a) extracted from the videos; (b) grayscale; (c) unsharp filter; (d) average filter; (e) Median filter; (f) close operation; (g) binarized; (h) opening operation; (i) edge detection evaluated.

Results and discussion

The experiments were carried out starting from Reynolds number of 8.6. For Reynolds numbers up to about 17.6, we could not observe any three-dimensional pattern. At higher Reynolds numbers, surface waves began to appear, yet without forming any particular pattern. A three dimensional free-surface pattern appeared not before at a Reynolds number of 32.3.

Copyright © 2019 and published by German Association for Laser Anemometry
GALA e.V., Karlsruhe, Germany, ISBN 978-3-9816764-6-4

Figure 5 shows some examples of the top view on the channel at different Reynolds numbers. In the pictures, the channel is centered. Flow is from top to bottom. Dark, vertical lines correspond to the sidewalls. The distance from the inflow is indicated with a measuring tape on the left. The bottom undulation in the channel appear as bright and dark horizontal bars in the picture, where the bright parts correspond to the areas with lowest local inclination angle. The three-dimensional surface pattern first appeared close to the sidewalls. It results in a modulation of the intensity distribution due to the bottom undulation, particularly of the bright regions. Apart from the steady three-dimensional pattern, surface waves can be identified in the lower part of the pictures, i.e. further downstream. They appear in the pictures as large-scale disturbances of the bottom pattern.

As indicates figure 5(a), the three-dimensional pattern first appears at the sidewalls near the inflow. Further downstream, it invades areas further away from the sidewalls, yet apparently without reaching the channel center. After having reached a maximum extension about 15 cm downstream of the inflow, the pattern shrinks again to a region close to the sidewalls. This seems to coincide with the occurrence of the traveling waves. As the Reynolds number increases, the three-dimensional pattern reaches the channel center and expands further downstream, see figure 5(b). At higher Reynolds number, the contrast caused by the three-dimensional pattern decreases, see also figure 5(c). That picture also shows that the three-dimensional pattern recedes to the sidewalls again at higher Reynolds numbers while traveling surface waves seem to be created in the channel center further upstream.

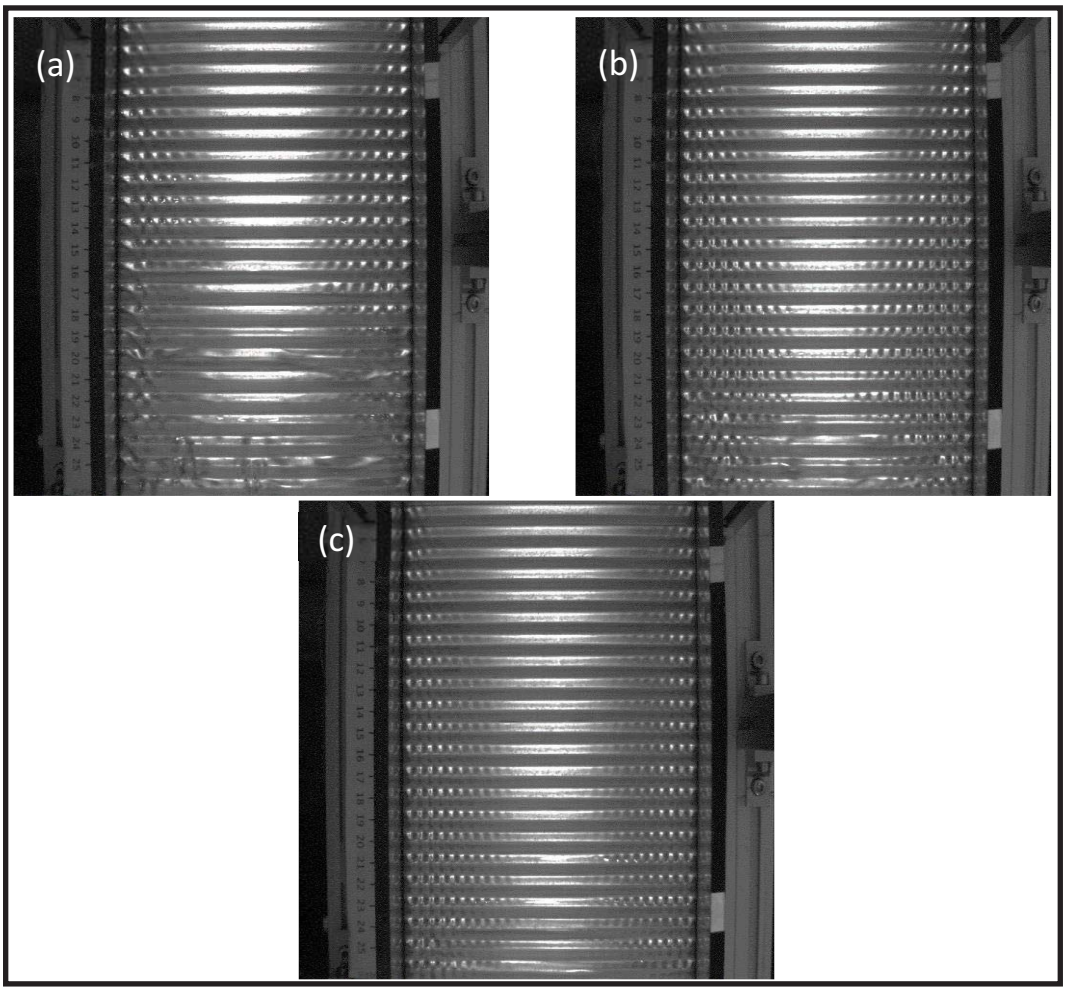

FIG. 5. Top views of the upstream part of the channel taken by shadowgraphy showing the three-dimensional patterns at three different Reynolds numbers: Re=32.3 (a), Re=37.8 (b), Re=43.1 (c).

Copyright © 2019 and published by German Association for Laser Anemometry
GALA e.V., Karlsruhe, Germany, ISBN 978-3-9816764-6-4

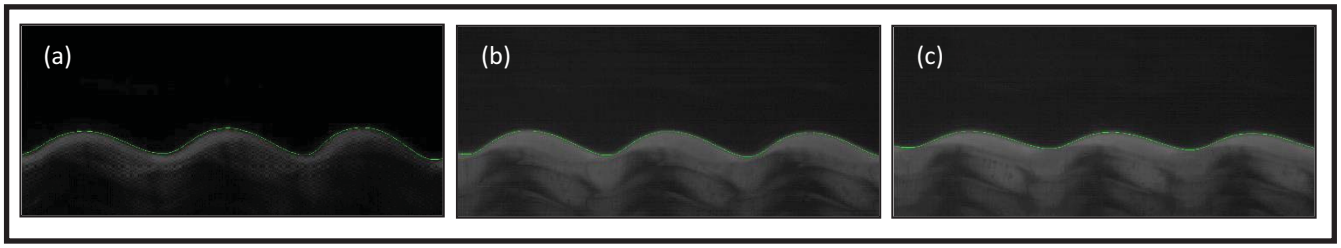

FIG. 6. Free-surface profile in main flow direction as detected with the light-sheet technique at three different Reynolds numbers: Re=32.3 (a), Re=37.8 (b), Re=43.1 (c). The green line indicates the detected free surface at the edge of the light sheet.

Wavelength in spanwise direction and amplitude of the pattern was determined with the light-sheet technique. Figure 6 shows examples of the surface profile in main flow direction at different Reynolds numbers. The free surface as extracted after image processing is indicated with a green line. Scanning the surface with the light-sheet technique, we recovered the free-surface contour of the pattern. Figure 7 shows an example of the surface pattern together with the bottom contour for in the area indicated in figure 3. Apart from the undulation in main flow direction that follows the bottom contour, there is a modulation in spanwise direction. The area depicted in the diagram covers about three such modulations. They are in phase between neighboring bottom undulations. One can distinguish a regular pattern of locations with undulations in streamwise direction of higher and lower peak-to-peak amplitudes that alternate periodically in spanwise direction. The locations of higher amplitudes show deeper valleys and higher crests. They are quite in phase with the bottom contour while those of lower amplitude appear with a phase shift upstream with respect to the bottom contour.

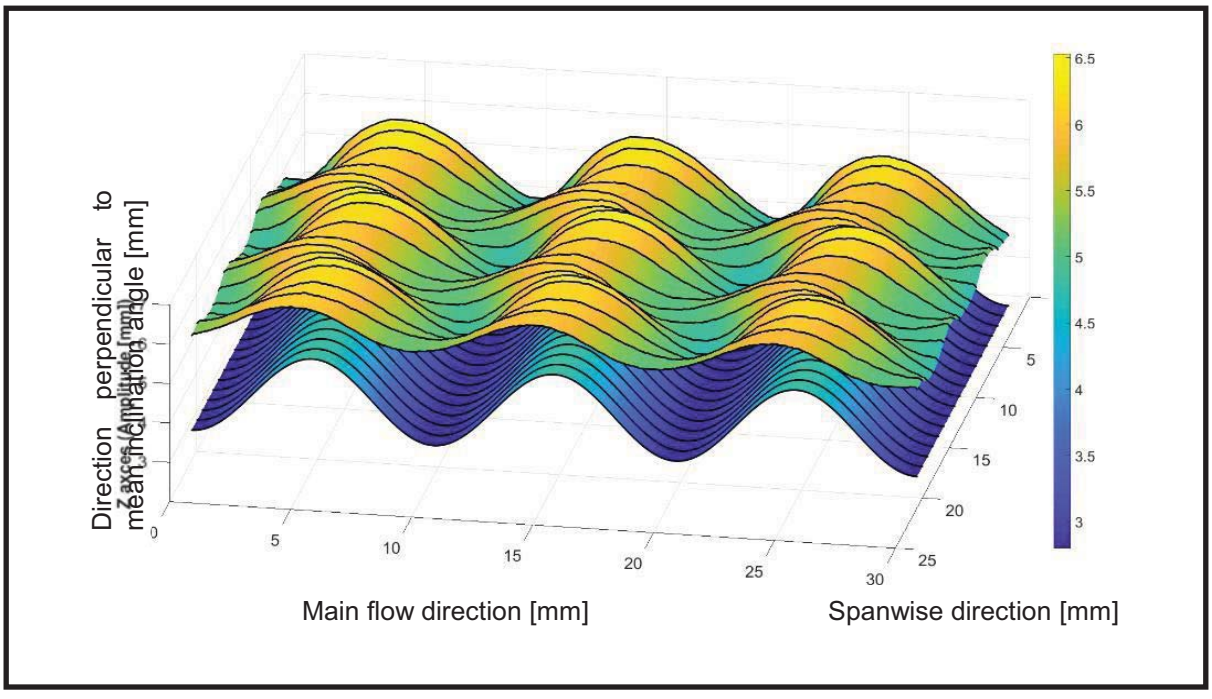

FIG. 7. Three-dimensional plot of the surface patterns at Reynolds numbers of 37.8. The height of the free surface from the image bottom is color-coded. Main flow direction is from left to right.

Copyright © 2019 and published by German Association for Laser Anemometry
GALA e.V., Karlsruhe, Germany, ISBN 978-3-9816764-6-4

Conclusions

We studied the formation of three-dimensional patterns on the free surface of a gravity driven film flow over a sinusoidal surface. We observed steady three-dimensional free surface patterns. We characterized their appearance and extension using shadowgraphy and quantified them with a light-sheet technique employing fluorescent dye.

References

N. Aksel and M. Schörner, 2018: "Films over topography: from creeping flow to linear stability, theory, and experiments, a review," Acta Mechanica 229, 1453-1482.
V. Bontozoglou and G. Papapolymerou, 1997: "Laminar film flow down a wavy incline", Int. J. Multiphase Flow 23, 69.
C. Heining, V. Bontozoglou, N. Aksel, A. Wierschem, 2009: "Nonlinear resonance in viscous films on inclined wavy planes", International Journal of Multiphase Flow 35, 78–90.
W. Schöpf, J. C. Patterson, A. M. H. Brooker, 1996: "Evaluation of the shadowgraph method for the convective flow in a side-heated cavity", Experiments in Fluids 21, 331-340.
M. Schörner, D. Reck, N. Aksel, 2015: "Does the topography's shape matter in general for the stability of film flows?", Physics of Fluids 27, 042103.
M. Schörner, D. Reck, N. Aksel, 2016: "Stability phenomena for beyond the Nusselt flow-Revealed by experimental asymptotics", Physics of Fluids 28, 022102.
A. Wierschem and N. Aksel, 2004: "Hydraulic jumps and standing waves in gravity-driven flows of viscous liquids in wavy open channels", Physics of Fluids 16, 3868.
A. Wierschem, V. Bontozoglou, C. Heining, H. Uecker, N. Aksel, 2008: "Linear resonance in viscous films on inclined wavy planes", International Journal of Multiphase Flow 34, 580-589.
A. Wierschem, C. Lepski, N. Aksel, 2005: "Effect of long undulated bottoms on thin gravity-driven films," Acta Mechanica 179, 41-66.
A. Wierschem and H. Linde, 2013: "*Shadowgraph contrast of internal wave trains during absorption",* in "*Without Bounds: A Scientific Canvas of Nonlinearity and Complex Dynamics"*, ed: R. G. Rubio *et al*., Springer, 363-370.
A. Wierschem, T. Pollak, C. Heining and N.Aksel, 2010: "Suppression of eddies in films over topography", Physics of Fluids 22,113603.
A. Wierschem, M. Scholle, N. Aksel, 2003: "Vortices in film flow over strongly undulated bottom profiles at low Reynolds numbers", Physics of Fluids 15, 426-435.

Copyright © 2019 and published by German Association for Laser Anemometry
GALA e.V., Karlsruhe, Germany, ISBN 978-3-9816764-6-4